Article Type: Letter

Multiple paths towards repeated phenotypic evolution in the spiny-leg adaptive radiation (*Tetragnatha;* Hawai i)

Running Title Repeated Phenotypic Evolution in spiny-legs

José Cerca[1,2,3,4,*], Darko D. Cotoras[5,6], Cindy G. Santander[7], Vanessa C. Bieker[3], Leke Hutchins[1], Jaime Morin-Lagos[3], Carlos F. Prada[8], Susan Kennedy[9], Henrik Krehenwinkel[9], Andrew J. Rominger[10], Joana Meier[11,12], Dimitar Dimitrov[13], Torsten H. Struck[2], Rosemary G. Gillespie[1]

1 - Berkeley Evolab, Department of Environmental Science, Policy, and Management, UC Berkeley, California, USA

2 - Frontiers in Evolutionary Zoology, Natural History Museum, University of Oslo, Norway

3 - Department of Natural History, NTNU University Museum, Norwegian University of Science and Technology, Trondheim, Norway

4 - Centre for Ecological and Evolutionary Synthesis (CEES), Department of Biosciences, University of Oslo, Oslo, Norway

5- Department of Terrestrial Zoology. Senckenberg Research Institute and Natural History Museum. Frankfurt am Main, Germany.

6- Department of Entomology. California Academy of Sciences. San Francisco, California, USA.

7 - Department of Biology, University of Copenhagen, Copenhagen, Denmark

8 - Grupo de Investigación de Biología y Ecología de Artrópodos, Facultad de Ciencias, Universidad del Tolima, Colombia

9 - Department of Biogeography, Trier University, Germany

10 - School of Biology and Ecology, University of Maine, USA.

11 - Department of Zoology, University of Cambridge, United Kingdom

12 - Tree of Life Programme, Sanger Insitute, Hinxton, United Kingdom

13 - Department of Natural History, University Museum of Bergen, University of Bergen, Postbox 7800, 5020 Bergen, Norway

* corresponding - jose.cerca@gmail.com

Keywords Parallel evolution, Convergent evolution, Araneae, Tetragnathidae, circadian rhythms, neuronal, melanin, genomic divergence, hybridization, introgression

Abstract

The repeated evolution of phenotypes is ubiquitous in nature and offers some of the clearest evidence of the role of natural selection in evolution. The genomic basis of repeated phenotypic evolution is often complex and can arise from a combination of gene flow, shared ancestral polymorphism and *de novo* mutation. Here, we investigate the genomic basis of repeated ecomorph evolution in the adaptive radiation of the Hawaiian spiny-leg *Tetragnatha*. This radiation comprises four ecomorphs that are microhabitat-specialists, and differ in body pigmentation and size (Green, Large Brown, Maroon, and Small Brown). Using 76 newly generated low-coverage, whole-genome resequencing samples, coupled with population genomic and phylogenomic tools, we studied the evolutionary history of the radiation to understand the evolution of the spiny-leg lineage and the genetic underpinnings of ecomorph evolution. Congruent with previous works, we find that each ecomorph has evolved twice, with the exception of the Small Brown ecomorph, which has evolved three times. The evolution of the

Maroon and the Small Brown ecomorphs likely involved ancestral hybridization events, whereas the Green and the Large Brown ecomorphs likely evolved because of either standing genetic variation or *de novo* mutation. Pairwise comparisons of ecomorphs based on the fixation index (F_{ST}) show that divergent genomic regions include genes with functions associated with pigmentation (melanization), learning, neuronal and synapse activity, and circadian rhythms. These results show that the repeated evolution of ecomorphs in the Hawaiian spiny-leg *Tetragnatha* is linked to multiple genomic regions and suggests a previously unknown role of learning and circadian rhythms in ecomorph.

Introduction

Adaptive radiation, the evolutionary process where an ancestral lineage diversifies into multiple phenotypically-distinct species which occupy different ecological niches, offers a natural experiment to disentangle links between the phenotypic diversification and environmental adaptation (Schluter 2000; Gillespie et al. 2020). Of particular interest in adaptive radiation is the repeated phenotypic evolution (i.e. parallel or convergent phenotypic evolution) (Cerca 2022), where equivalent phenotypes evolve in response to similar ecological challenges (Losos and Ricklefs 2009; Losos 2010). Repeated evolution of similar phenotypes has been found in multiple radiations and offers a powerful approach for disentangling recurrent and potentially-deterministic phenotypic outcomes in response to similar environmental conditions (Losos 2010, 2011; Gillespie et al. 2018, 2020; Malinsky et al. 2018; Salzburger 2018; Masonick et al. 2022; Urban et al. 2022). For instance, the repeated evolution of habitat-specialists, termed ecomorphs, has been reported in multiple adaptive radiations including the Caribbean *Anolis* lizards (Losos and Ricklefs 2009) and Hawaiian *Tetragnatha* (Gillespie 2004) and *Ariamnes* (Gillespie et al. 2018) spiders. In these cases, the repeated evolution of ecomorphs has been explained based on the spatial segregation of environments, as different islands offer similar environmental conditions (Losos and Ricklefs 2009; Losos 2010). However, despite the deluge of genomic data, and new insights into phenomena of admixture,

73 epigenetics, and other phenomena that highlight the overall flexibility of the genome, we know
74 little about the genomic underpinnings involved in the evolution of discrete phenotypes that
75 appear to arise repeatedly in response to similar selective pressures. The current study set out
76 to examine the genomic basis of recurrent ecomorph evolution in a lineage of Hawaiian spiders.
77

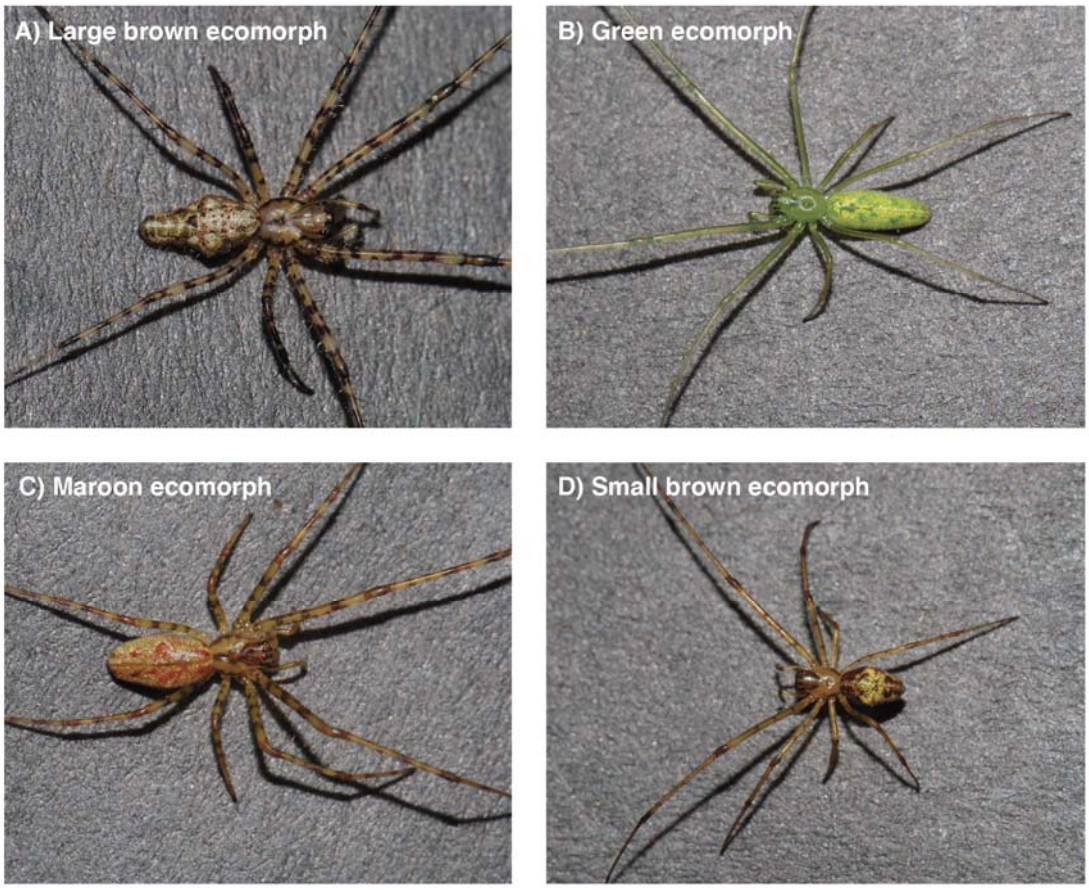

78

79 **Figure 1.** ***Tetragnatha*** **spiny-leg ecomorphs** including representatives of (A) the Large Brown
80 (*Tetragnatha quasimodo*), (B) the Green (*Tetragnatha brevignatha*), (C) the Maroon
81 (*Tetragnatha kamakou*), and (D) the Small Brown (*Tetragnatha anuenue*). Photographs by
82 Darko D. Cotoras.

83

The Hawaiian *Tetragnatha* spiny-leg species belong to a clade comprising ~17 species, and are part of a large radiation endemic to the archipelago (Gillespie 2016; Kennedy et al. 2022). These species can be grouped into four ecomorphs (Figure 1 A-D), which are linked to the substrate they inhabit (Gillespie 2004): the Large Brown ecomorph is found on tree bark (Figure 1A), the Green ecomorph on leaves (Figure 1B), the Maroon ecomorph on mosses (Figure 1C), and the Small Brown ecomorph on twigs (Figure 1D). Ancestral character-state reconstructions suggest that the Green ecomorph is likely the ancestral form, having evolved once, while the remaining ecomorphs each evolved twice (Gillespie 2004). Recent genomic work has shown that co-occurring closely related species belonging to the Green ecomorph do not hybridize, and it has been argued that there may be some overlap in their ecological niches in the early stages of diversification, suggesting a possible avenue for the divergence of ecomorphs through character displacement upon secondary contact (Schluter 2000; Cotoras et al. 2018). The genomic bases of ecomorph evolution, which will allow for the ecological differentiation of these closely related and ecologically equivalent species are still poorly understood.

The repeated evolution of a phenotype can arise as a result of three non-mutually exclusive genomic processes (Stern 2013; Pease et al. 2016; Lee and Coop 2017, 2019): *de novo* mutation (different mutations causing similar phenotypes), shared ancestral polymorphism (standing variation, old genetic variation being re-recruited), or hybridization (where a particular allele is recruited from one lineage to another). All three patterns have been observed in the context of adaptive radiations (Meier et al. 2018; Choi et al. 2021; Sowersby et al. 2021; De-Kayne et al. 2022). Because they leave distinct footprints along the genome, genomic-level data is able to tease apart the contribution of each of these processes (Lee and Coop 2017).

Here, we whole-genome re-sequence 76 genomes across the *Tetragnatha* spiny-leg radiation with the aim of understanding the genomic basis of repeated ecomorph evolution. We hypothesise that standing genetic variation has been the source for phenotypic repetition in *Tetragnatha* spiny-legs. We start by reconstructing the evolutionary history of the spiny-leg

lineage using phylogenetic tools. Then, we explore patterns of excess allele sharing to infer potential hybridization. Finally, we investigate genomic divergence (F_{ST}) to understand differentiation between ecomorphs. Our results uncover a complex evolutionary history, showing that repeated evolution may have emerged through multiple different genomic processes.

Methods

Field collection

Spiny-leg *Tetragnatha* live in the montane rain forests of all the major Hawaiian islands (1,200-1,800 meters) (Roderick et al. 2012). Specimens were collected either by hand (at night, when spiders are active) or using a beating sheet (both day and night). Specimens were preserved in 95% ethanol and stored at -20°C. A list of specimens including their volcano and island is found in Supplementary Table 01.

Molecular data generation

We sequenced genomes from a total of 76 individuals (Supplementary Table 01). For each specimen, we extracted DNA from 2-4 legs. Legs were first ground using a tube pestle and incubated overnight in a solution of lysis buffer (10mM Tris pH, 100mM NaCl, 10mM EDTA, 0.5% SDS) and proteinase K at 54° C, we then followed the instructions of the commercial provider Qiagen to extract the DNA. We diluted the DNA in 50 µl of elution buffer and assessed the DNA concentration of each of the 76 extracts using a Qubit fluorometer (ThermoFisher).

Samples with more than 500 ng of DNA were submitted to the QB3-Berkeley, Vincent J. Coates Genomics Sequencing Laboratory at UC Berkeley, where library preparation was conducted. DNA was fragmented using a Bioruptor Pico (Diagenode) and libraries prepared using the KAPA Hyper Prep kit for DNA (KK8504). This involved adding truncated universal stub adapters for DNA-adapter ligation, and indexed primers for PCR amplification (to complete

the adapters). The quality of the samples was checked on an AATI (now Agilent) Fragment Analyzer, and the molarity of the library was measured using quantitative PCR with the KAPA Library Quantification Kit (Roche KK4824) on a BioRad CFX Connect thermal cycler. Libraries were then pooled by molarity and sequenced on an Illumina NovaSeq 6000 S4 flowcell for 2 x 150 cycles, with the aim of obtaining 10 Gbp per sample (~9.5x sequencing depth of the genome). Raw sequencing data was converted to FASTQ format and demultiplexed using the Illumina bcl2fastq2 software while allowing for up to one mismatch in the index sequences.

Bioinformatics data processing

All of the steps below are reported in GITHUB JOSE. We checked the quality of the sequencing data using fastQC v0.11.8 (Andrews 2017), and identified adapters using AdapterRemoval v2.3.1 (--identify-adapters) (Schubert et al. 2016). We then used Trimmomatic v0.39 (Bolger et al. 2014) to remove adapters and poor quality reads by specifying: maximum 2 mismatches in the adapter sequence; cut three base pairs in the beginning and the end of the read if the quality drops below 20 in these regions; a sliding window of 4 bp with a minimum quality threshold of 20, and a minimum read length of 50. These high-quality reads were aligned to the *Tetragnatha kauaiensis* reference genome v1 (~1.1 Gb) (Cerca et al. 2021a) using the Burrows-Wheeler Aligner v0.7.17, mem algorithm (Li and Durbin 2009). Because Trimmomatic separates reads as forward-paired, reverse-paired, forward-unpaired, and reverse-unpaired, we aligned all four files to the reference genome, and merged and sorted the final file using Samtools v1.10 (Li et al. 2009). We then estimated mapping quality of each alignment using samtools flagstat, finding no mapping-bias (Supplementary Table 01), and marked duplicates using GATK 4.1.4.0 (McKenna et al. 2010), by running the SortSam algorithm which sorted reads based on genomic coordinates, followed by the MarkDuplicates function. We then built indexes for each alignment using BuildBamIndex (McKenna et al. 2010), and filtered reads with a low mapping quality (MAPQ) using samtools. Specifically, we discarded reads with mapping quality below 30, and calculated the sequencing depth using samtools depth (option -a was used

to output all sequencing positions, even those with 0 depth; Supplementary Table 01). We then processed the data using ANGSD v0.935 (Kousathanas et al. 2017), a pipeline designed to handle and analyze low coverage sequencing data.

Phylogenetic analyses

We started by doing a phylogenetic reconstruction while accounting for low-coverage to understand the ancestral relationships of ecomorphs. As part of this analysis, we included five specimens from four species belonging to an outgroup lineage, the *Tetragnatha* web builder radiation, which is also endemic to Hawai'i (*Tetragnatha maka*, *Tetragnatha acuta*, *Tetragnatha filiciphilia*, and *Tetragnatha stelarobusta*). We started by calling variants in ANGSD using the GATK genotype likelihood model to output a beagle file (-GL 2 -doGlf 2), specifying that a variant should be present in at least 38 individuals (half of the dataset), minimum base quality of 30 (-minQ), a *p*-value threshold of 1e-6 (-SNP_pval), to remove allele counts in less than 5% of the dataset (-minMaf 0.05), and to infer major and minor alleles from the genotype likelihoods (-doMajorMinor 1). The output beagle file was then processed using an in-house script to remove variants in repeat regions by downloading the general feature format file (gff3) from (Cerca et al. 2021a), including the genomic location of repeat elements, converting it to a bed file format using bedtools v2.26.0 (Quinlan and Hall 2010), and generating a white-list of the genome (i.e. non-repeated genomic areas) using an in-house script (See Github). This dataset was used as input in NgsDist (Vieira et al. 2015), where we specified a block size of 20 SNPs, and 100 bootstrap replicates. We then ran the NJ software fastme v2 (Lefort et al. 2015), merged all the 100 replicates into a final tree with bootstrap support using RAXML while specifying an optimization of branch-length, and specifying GTRCAT (GTR + Optimization of substitution rates + Optimization of site-specific) as the substitution model.

Because different parts of the genome can have different topologies as a result of different evolutionary mechanisms, we additionally performed a mitochondrial phylogenetic

reconstruction and a phylogenetic reconstruction based on Ultra Conserved Elements (UCE). We retrieved mitochondrial genomes and did a tree reconstruction to analyse nuclear-mitochondrial discordances; which are typically associated with hybridization events. We started by extracting the mitochondrial genomes from the cleaned Illumina libraries using Novoplasty v4.2 (Dierckxsens et al. 2017), a method which uses an iterative baiting-and-expand approach to construct genomic regions. We obtained a collection of seeds encompassing different mitochondrial genes (16S rDNA (hereafter 16S), Cytochrome Oxidase I (COI), and Cytochrome B (CytB)) for species from the radiation (Kennedy et al. 2022). For each specimen, we ran all seeds until we obtained a circularized mitochondrial genome. If no complete mitochondrial genome was obtained for a given specimen, we took the longest contig obtained by Novoplasty. In total, we obtained 46 complete fully-circularized mitochondrial genomes, and 19 partially complete mitochondrial genomes (>5,000 bp). We then concatenated and aligned the 65 mitogenomes using Mafft v7.130b (Katoh and Standley 2013), trimmed the ends of the alignments and ran a tree using IQ-Tree v2.0.3 specifying 1,000 ultrabootstrap replicates and automatic determination of substitution models.

We obtained a UCE dataset to complement the ngsDist methods with a maximum likelihood-based analysis. For each sample, we started by calling every position of the genome using the Bcftools' v1.10.2 mpileup and call algorithms (Danecek et al. 2021), using the *T. kauaiensis* genome v1 as reference. The output files were normalized for indels using bcftools norm, and filtered for gaps bigger than 4 base pairs, base quality above 20, depth above 1 and below 30. These files were then turned into consensus fasta sequences using bcftools consensus. To extract UCEs from these consensus files, we used the phyluce pipeline (Faircloth 2016), with the 'Arachnida-UCE-1.1K-v1' set as bait. Phyluce allows extraction of UCEs, but because of the missing data due to low coverage and fragmented genomes, we were only able to retrieve 29 UCEs that were present in half of the dataset (16 of the UCEs were present in all individuals; and 23 UCEs present in ≥70 individuals).

Partitioning of genetic variation and hybridization

After reconstructing species and ecomorph relationships we analysed the partitioning of genetic variation and whether hybridization has occurred in the radiation. We studied the partitioning of genetic variation by running a NGSAdmix analysis. This analysis required processing the data with ANGSD, similar to the one used for the phylogenetic reconstruction with NgsDist, but with three exceptions. Specifically, we included a minimum base quality of 20 (-minQ) filter, removed variants with a minimum allele frequency of 0.05 (-minMaf 0.05), and inferred major and minor alleles (-doMajorMinor 1). After filtering for variants in repeat regions, we filtered the data for severe deviations from the Hardy-Weinberg equilibrium (HWE) using PCAngsd, which estimated a likelihood ratio test (LTR) to identify sites where severe deviations of the HWE occur (LTR >24, following recommendations from the contributors of ANGSD; https://github.com/GenisGE/grantsGazelleScripts) (Garcia-Erill et al. 2021). Additionally, given that admixture-like analyses assume that variants are independent, we implemented a linkage disequilibrium (LD) filter. This was done by calculating LD in windows of 100,000 bps using plink (Purcell et al. 2007) and using an in-house script explore LD-decay. We LD-pruned the data by removing genomic regions where linkage, measured as R2, was above 0.11 in windows of 25,000 bps (5,000 bp steps). We then ran NGSadmix analyses (Skotte et al. 2013). We specified cluster values *(K)* between 1-20, and for each we performed 10 independent runs until each reached chain convergence. We estimated the best K to be 2 using the Evanno method (Evanno et al. 2005) as implemented as part of CLUMPAK (Kopelman et al. 2015). We present the results for K=2, 3, and 15 as ADMIXTURE plots help to clarify how genetic variation is partitioned at different levels (Meirmans 2015).

Considering the nuclear-mitochondrial discordance, we calculated excess of shared alleles in the dataset. To do so, we re-ran ANGSD, with the parameter specification as adone for the NGSadmix analyses, further specifying a genotype likelihood depth filter between 7 and 30 (-geno_minDepth 7 -geno_maxDepth 30). The outputted genotype file was processed to remove variants in repeat regions and the excess allele sharing was calculated using Patterson's D

(ABBA-BABA) and *F*4 ratios (Patterson et al. 2012) using Dsuite (Malinsky et al. 2021). Both these analyses benefited from a tree-backbone and we specified the tree obtained in ngsDist.

Scans of selection

Whole-genome level data allows understanding whether certain genes or genomic regions are under selection as this process leads to shifts in allelic frequencies (Ravinet et al. 2017). In order to calculate population differentiation (F_{ST}), we obtained the Site Frequency Spectrum (SFS) using ANGSD. As our goal is to understand the evolution of ecomorphs, we analysed the data for each monophyletic ecomorph group, based on the nuclear phylogenetic reconstruction obtained with NGSdist. Furthermore, because SFS and F_{ST} estimations require allelic frequencies from multiple individuals, we selected only ecomorphs with 5 or more specimens (Supplementary Table 01). To obtain SFS estimates we ran ANGSD separately for: *Tetragnatha pilosa* (Large Brown group A), *T. quasimodo* (Large Brown group B), *T. kauaiensis* (Green group A), *T. tantalus*, *T. polychromata*, *T. brevignatha*, *T. waikamoi* (Green group B), *T. obscura*, *T. kukuiki*, *T. kikokiko*, *T. anuenue* (Small Brown ecomorph), and *T. kamakou* (Maroon ecomorph). We ran ANGSD independently for each of these groups, specifying that loci had to be in at least 5 individuals, keeping only reads with a single mapping (-uniqueOnly), discarding bad reads (-remove_bads), and keeping variants with a minimum base quality of 20. This yielded a 1-dimensional SFS for each population, which was then processed using realSFS (using -fold 1) to obtain 2-dimensional SFSs for the following pairs: the two Large Browns (Large Brown A vs Large Brown B), the two Greens (Green A vs Green B), Green vs Maroon (Green B vs Maroon), and Small Brown vs Large Brown (Small Brown vs LargeBrown B). For each of the 2-dimensional SFS, we ran the realSFS F_{ST} index algorithm, followed by realSFS F_{ST} stat to obtain the overall F_{ST}. Because we were interested in identifying genomic areas of divergence and loci within, we ran the realSFS F_{ST} stat2 algorithm to obtain F_{ST} in 5,000 bp non-overlaping windows. We identified regions of differentiation by Z-transferring F_{ST} and using a Z cut-off of >3. After identifying significantly differentiated regions, we retrieved genes for these windows from the

gene annotations of the *T. kauaiensis* genome (Cerca et al. 2021a). We then called orthologs between *T. kauaiensis* and the *Drosophila melanogaster* genome annotations to obtain evidence on gene function, benefiting from the decades of functional genetic research on the latter, using *OrthoFinder2* (Emms and Kelly 2015). After identifying the closest *D. melanogaster* ortholog for a particular gene on a region with high differentiation, we reviewed and summarized the literature on that gene in Supplementary Table 2. When possible, we read at least three papers for each gene.

Hybridization along the genome

We found evidence for hybridization, and because this process can leave tracks along the genome, we performed an analyses to understand the breadth and impact of hybridization on the genomes. Specifically, the results showed a strong signal of admixture between *T. kamakou* (Maroon ecomorph), *T. perreirai* (Maroon ecomorph), and *T. restricta* (light Brown ecomorph) and to understand whether hybridization occurred we did a TWISST analysis on the three biggest scaffolds and D-suite investigate for the scaffolds with melanization genes. For the TWISST analysis, we selected *T. anuenue*, *T. perreirai*, *T. restricta*, and *T. mohihi*. We started by running ANGSD for non-overlapping regions of 5kb segments of the genome, specifying a minimum map quality of 30, minimum base quality of 20, outputting the frequency of the different bases. We then did a NJ-tree for each of these regions using the R package ape (Paradis et al. 2008). We then ran TWISST specifying *T. anuenue*. For the windowed Patterson's D, we used Dsuite investigate on the scaffolds with melanization genes.

Results

289 Tree reconstruction

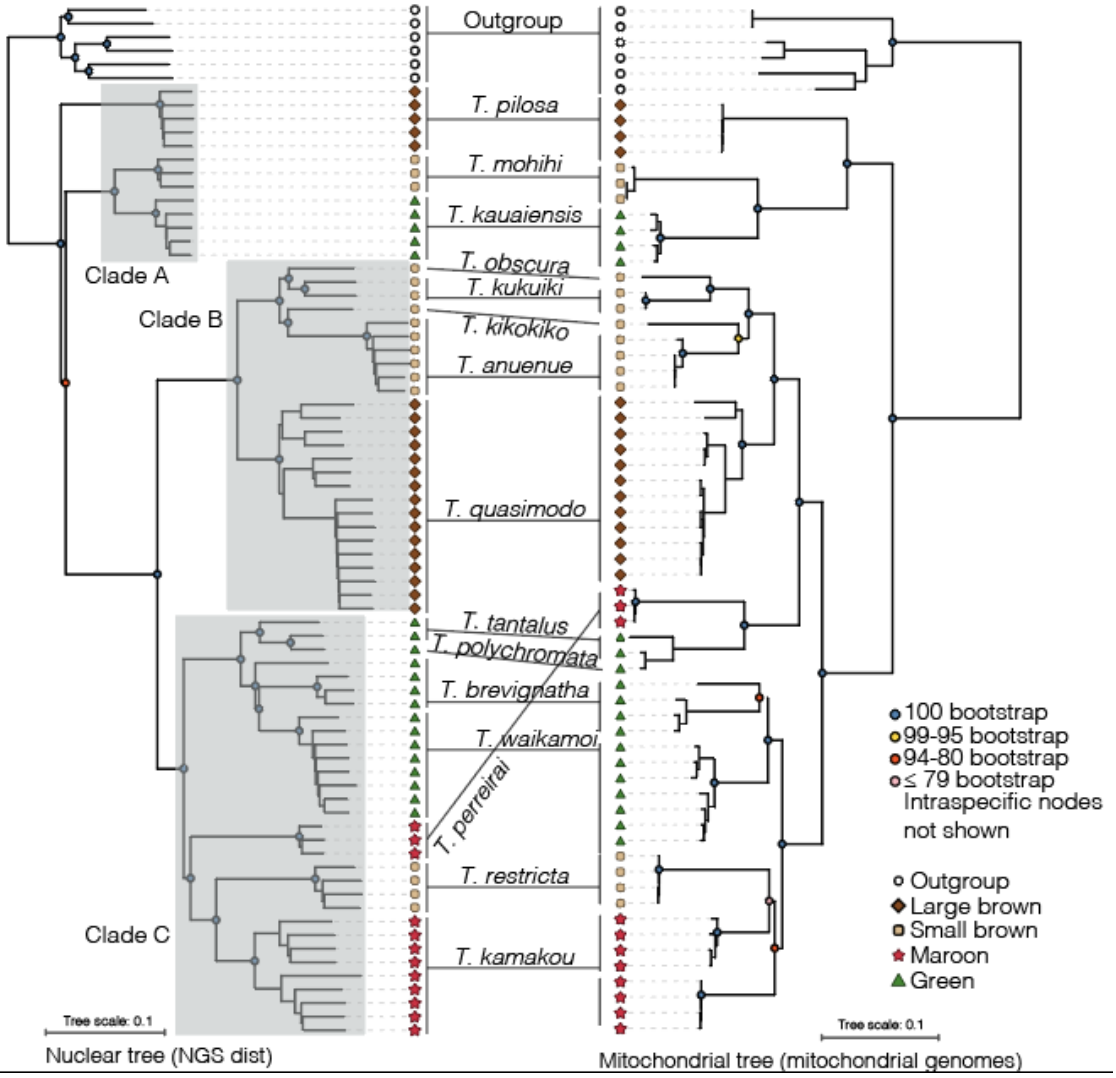

290

291 **Figure 2. Nuclear and mitochondrial tree reconstructions** The nuclear tree (left) obtained by
292 NgsDist is based on 1,848,915 variable sites. The mitochondrial tree (right) obtained by
293 NovoPlasty and IQ-Tree is based on complete and partial mitochondrial genomes. Bootstrap is
294 provided for each inter-specific node, and the tips of the phylogeny include ecomorph and
295 outgroup labelling as coloured symbols. Clades A-C are plotted in the nuclear tree.

296

In the nuclear tree, *T. pilosa* is sister to the remaining spiny-leg species. The node including all other spiny-legs, however, has a bootstrap support below 95, while all other interspecific nodes have a bootstrap support of 100. Furthermore, the node including all spiny-legs but *T. pilosa* is preceded by a very short branch, and separates two clades: one clade including *T. mohihi* and *T. kauaiensis*, and another clade with all remaining species. The remaining species can be separated in two major clades, the first (clade B) including the Large Brown *T. quasimodo* and a group of Small Brown species including *T. obscura*, *T. kukuiki*, *T. kikokiko*, *T. anuenue*; and the second (clade C) including a group of species representing the Green ecomorph (*T. tantalus*, *T. polychromata*, *T. waikamoi, T. brevignatha*), which is sister to a group comprising two Maroon species (*T. perreirai* and *T. kamakou*) and a Small Brown species (*T. restricta*). The maximum-likelihood UCE tree is topologically concordant with the ngsDist tree at the ecomorph level (Supplementary Figure 01). The only topological discordance is the species' placement within the Small Brown group as part of clade B (*T. obscura*, *T. kukuiki*, *T. kikokiko*, *T. anuenue*). Specifically, the ngsDist tree (Figure 2) shows *T. kukuiki* as sister to *T. obscura*, and *T. kikokiko* as sister to *T. anuenue*, whereas on the UCE tree, *T. anuenue* is sister to a clade including all the aforementioned species (Supplementary Figure 01).

There are mitochondrial-nuclear tree discordances based on topology and bootstrap support (Figure 2). First, in the mitochondrial tree, *T. pilosa* groups together with *T. mohihi* and *T. kauaiensis*, forming a clade while *T. pilosa* branches separately in the nuclear tree. Notably, all basal interspecific nodes have a bootstrap support of 100. Second, *T. tantalus* and *T. polychromata* (Green ecomorphs) are sister to *T. perreirai* (Maroon ecomorph) in the mitochondrial tree, and the clade comprising these three species is sister to the clade including the Large Brown (*T. quasimodo*) and the Small Brown ecomorphs (*T. obscura*, *T. kukuiki*, *T. kikokiko*, *T. anuenue*). These also have 100 bootstrap support at the relevant interspecific nodes. The mitochondrial tree shows that the evolution of Green ecomorphs has occurred three times (1 - *T. kauaiensis;* 2 - *T. tantalus* and *T. polychromata*; 3 - *T. waikamoi* and *T. brevignatha*), as opposed to two clades in the nuclear tree (1 - *T. kauaiensis;* 2 - *T. tantalus*, *T. polychromata*,

T. waikamoi and *T. brevignatha*). Third, the mitochondrial dataset shows *T. kamakou* as paraphyletic, separating the populations from Moloka□i and Maui (East Maui volcano). However, this node is weakly supported as it has a bootstrap value below 80.

For simplicity, and based on the mitochondrial phylogenetic reconstruction (and ngsAdmix below), we refer to clades A (*T. kauaiensis*, *T. pilosa*, *T. mohihi*), B (*T. anuenue*, *T. obscura*, *T. kukuiki*, *T. kikokiko*, *T. quasimodo*) and C (*T. kamakou*, *T. restricta*, *T. perreirai, T. tantalus, T. polychromata, T. waikamoi and T. brevignatha*) hereafter.

Structuring of genetic diversity

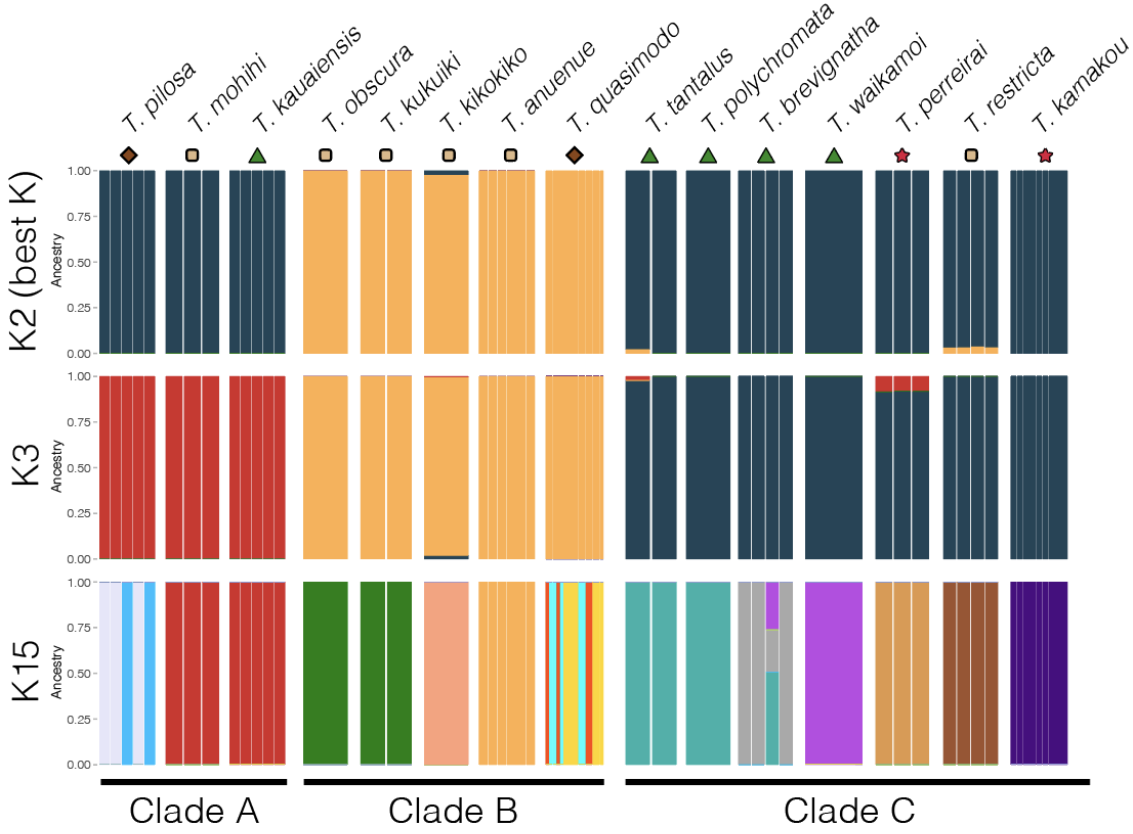

336 **Figure 3. Structure of genetic diversity** NgsAdmix analysis with cluster (*K*) values of 2 (best *K*), 3
337 (major clades), and 15 (number of species).

338

339 The best *K* obtained by the Evanno method was $K = 2$ (Figure 3). This *K* separated clade
340 B from the remaining clades (A and C), while $K = 3$ separated all three clades obtained in the
341 phylogeny. There is evidence of a shared history for both *K* values, some species having minor
342 components of other clades. For instance, *T. kikokiko* (Clade B) has a minor component of
343 ancestry from clades A-C on $K = 2$, and a minor component from clade C on $K = 3$. We also
344 display $K = 15$ because that is the number of species in the dataset (Figure 3). For $K = 15$, some
345 species are assigned to the same genetic cluster: *T. kauaiensis* and *T. mohihi* (red), *T. obscura*
346 and *T. kukuiki* (green), and *T. polychromata* and *T. tantalus* (aqua-blue). Two species,
347 interestingly both Large Browns, have intra-specific population structure (*T. pilosa* has two
348 colours, while *T. quasimodo* has three). Only one *T. brevignatha* sample has mixed ancestries, all
349 in common with species belonging to the Green ecomorph.

350

351

352

353 Excess allele sharing

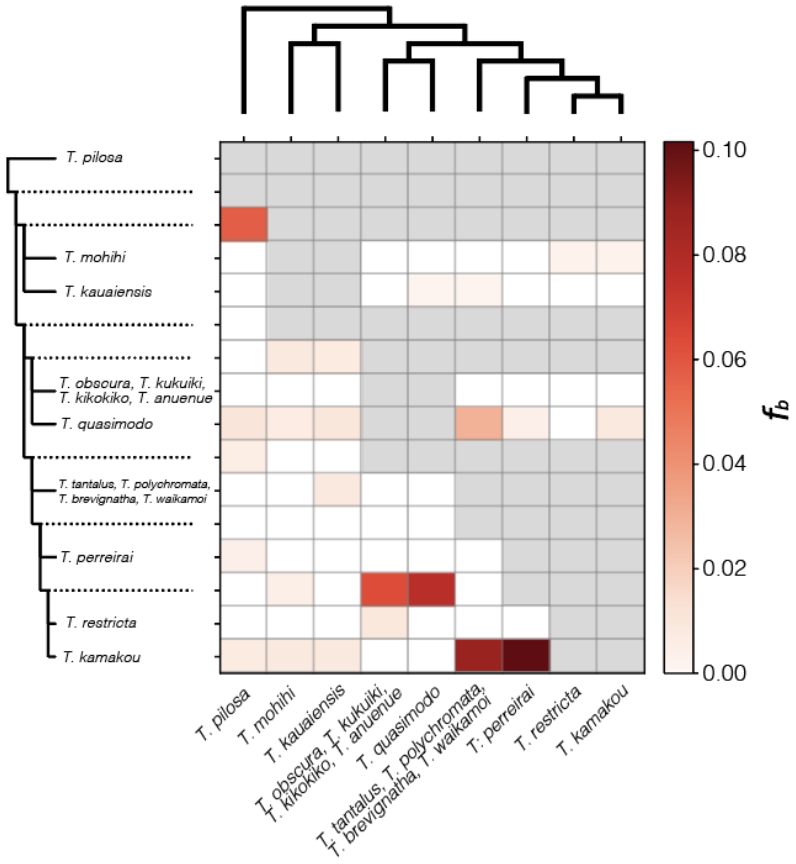

354

355 **Figure 4. Excess allele sharing** F4-branch statistic plotted as a heatmap. The tree topology
356 obtained by NgsDist and UCEs is plotted above and on the left every branch of the tree is
357 displayed (including internal branches). Because the goal is to understand hybridization
358 between ecomorphs, clades of closely related species belonging to the same ecomorph (i.e.
359 monophyletic ecomorphs) are displayed.

360

361 Based on Patterson's D statistics (Supplementary Figure 02) and F4-branch statistics,
362 we found excess allele sharing between ecomorphs and within ecomorphs (Figure 4). We
363 detected the largest excess in allele sharing between the Maroon ecomorph species (*T. perreirai*
364 and *T. kamakou*; the trio P1 = *T. restricta*; P2 = *T. kamakou*; P3 = *T. perreirai* had a D-statistic

of 0.15, Z-score 30.42 over >150,000 sites). In the Small Brown ecomorph, we also detected excess allele sharing, specifically between *T. restricta* and the remaining species (Figure 4; the trio P1 = *T. perreirai*; P2 = *T. restricta*; P3 = *T. obcura-kukuiki-kikokiko-anuenue* trio had a D-statistic of 0.13, Z-score of 8.21; >150,000 sites; Supplementary Table 03). No evidence for excess allele sharing was found between Green and Large Brown ecomorphs (Figure 4). When comparing ecomorphs, we find evidence of excess allele sharing between the lineages of clade A, namely between *T. pilosa* (Large Brown ecomorph), and *T. kauaiensis* and *T. mohihi* (Small Brown ecomorph); there is also excess of allele sharing between the Green ecomorph group (*T. tantalus*, *T. polychromata*, *T. brevignatha*, *T. waikamoi*) and one of the Maroon ecomorph species (*T. kamakou*). The Large Brown species *T. quasimodo* had excess allele sharing with the clade consisting of *T. restricta* (Small Brown ecomorph) and *T. kamakou* (Maroon ecomorph).

The windowed-analyses of D-statistics and TWISST showed no particular pattern of introgression for *T. restricta*, *T. kamakou* and *T. perreirai*. Specifically, D-statistics of regions where melanization genes were found (see F_{ST} scans below) were not elevated. The TWISST analyses showed no specific tracks of hybridization in the largest three scaffolds (Supplementary Figures 3-5).

381

F_{ST} scans

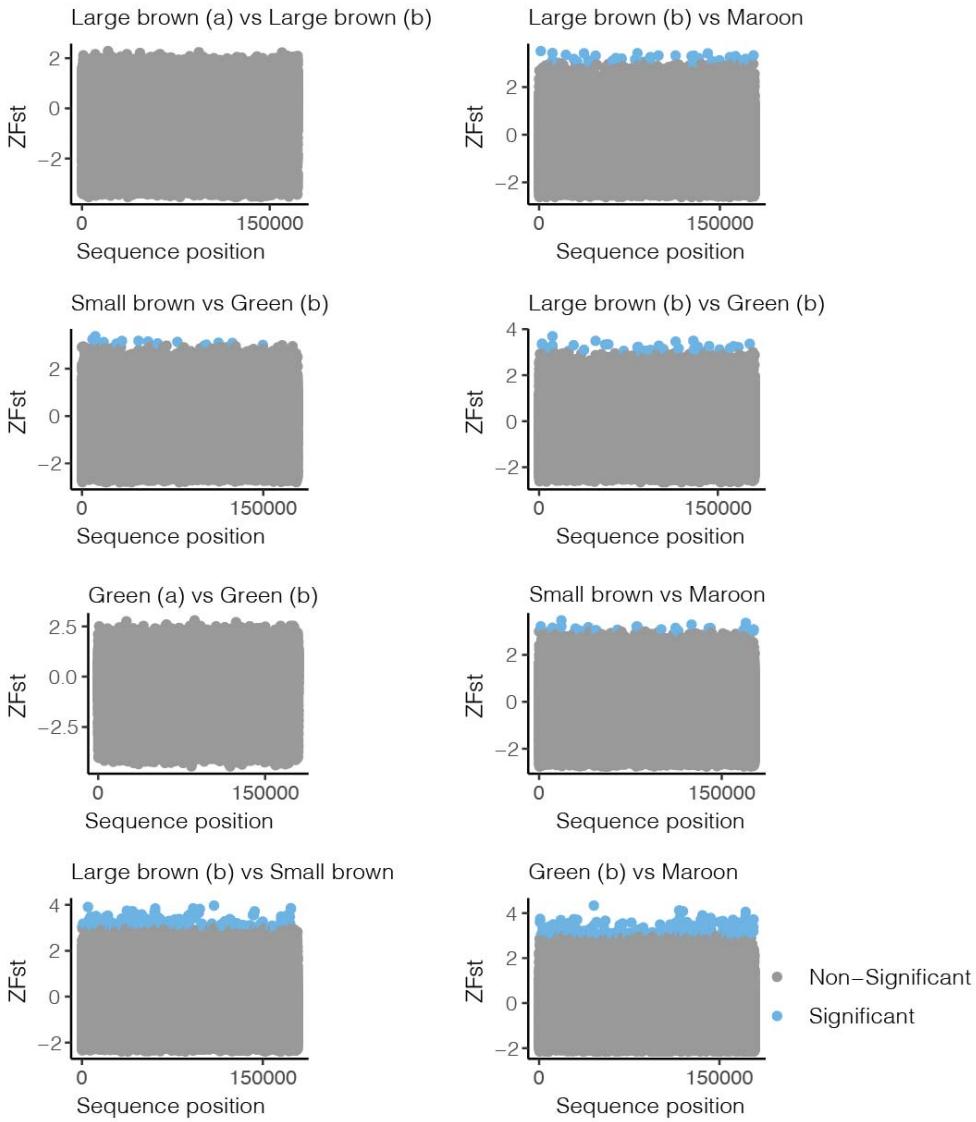

382

Figure 5. F_{ST} Scans of genomic divergence For each pairwise comparison, we provide the sequence position and a Z-transformed F_{ST} value. Significant Z values are displayed in blue ($Z > 3$) and non-significant in grey. Large Brown (a) includes *T. pilosa* (5 individuals); Large Brown (b) includes *T. quasimodo* (16 individuals); Green (a) includes *T. kauaiensis* (5 individuals); Green (b) includes *T. tantalus*, *T. polychromata*, *T. brevignatha*, *T. waikamoi* (15 individuals); Small Brown includes *T. obscura*, *T. kukuiki*, *T. kikokiko*, *T. anuenue* (10 individuals); Maroon includes *T. kamakou* (9 individuals).

We ran F_{ST} comparisons for lineages with five or more individuals (Figure 5). The two within-ecomorph comparisons (i.e. Large Brown (a) *vs* Large Brown (b); Green (a) *vs* Green (b)) yielded no significant F_{ST} outliers, and this is likely attributed to the overall high F_{ST} between more distantly related species in the radiation (Large Brown (a) *vs* Large Brown (b) had an global F_{ST} of 0.60; Green (a) *vs* Green (b) had an global F_{ST} of 0.61). The remaining comparisons, displayed in Figure 5, all had overall F_{ST} between 0.31 (Green (b) *vs* Maroon) - 0.41 (Small Brown *vs* Maroon).

Several areas of divergence along the genome seem to be common in pairwise comparisons. Specifically, while significant F_{ST} can be driven by a highly divergent region in a single lineage, we found that multiple regions of the genome seem to be commonly differentiated. For example, we found twelve genomic regions where significant F_{ST} values were identified in different pairwise comparisons. As an example, the region between 10,000 - 15,000 bp on Scaffold-2,488 had F_{ST} outliers when comparing Large Brown (b) *vs* Green (b) and Small Brown *vs* Maroon.

Table 1 Summary of genes in areas with high genomic divergence (F_{ST}).

Comparison	Gene	Function	References

Large Brown (b) vs Green (b)	NAT1	Circadian rhythm	(Bradley et al. 2012)
Large Brown (b) vs Green (b)	ALT	Neuron feeding source	(Volkenhoff et al. 2015)
Large Brown (b) vs Green (b)	Dscam	Immune-response associated	(Nazario-Toole et al. 2018)
Large Brown (b) and Small Brown	Mal-B1	Starch digestion	(Wu et al. 2016)
Large Brown (b) and Small Brown	vhaSFD	Longevity and life span	(Paaby and Schmidt 2009; Proshkina et al. 2015)
Large Brown (b) and Small Brown	Ank	Synaptic activity	(Koch et al. 2008)
Large Brown (b) and Small Brown	NAT1 and Gnpnat	Circadian rhythm	(Mattila and Hietakangas 2017)
Large Brown (b) and Small Brown	CG8483, and anon-WO0118547.80	Melanization-associated	(Bastide et al. 2016)

Large Brown (b) and Small Brown	CG8483	Posterior development genes	(Ibrahim et al. 2013)
Large Brown (b) and Maroon	ND-B17 and ALT	Synapsis	(Ghosh 2013)
Large Brown (b) and Maroon	NAT1, MFS10, and Period circadian protein	Circadean rythm	(Curtin et al. 1995; Fernandez-Chiappe et al. 2021)
Large Brown (b) and Maroon	LIMK1	Learning and memory formation	(E. A. Nikitina, A. V. Medvedeva, Yu. F. Dolgaya, L. I. Korochkin, G. V. Pavlova & E. V. Savvateeva-Popova 2012)
Green (b) and Maroon	CG18473	Growth-regulation	(Hevia et al. 2017)
Green (b) and Maroon	Syp, CG8545, and Trpgamma	Synapses, neurojunctions, neurons and nervous-system related	(Guan et al. 2005; Liebl et al. 2006; Yang et al. 2017)
Green (b) and Maroon	LIMK1	Learning and memory formation	(E. A. Nikitina, A. V.

			Medvedeva, Yu. F. Dolgaya, L. I. Korochkin, G. V. Pavlova & E. V. Savvateeva-Popova 2012)
Green (b) and Maroon	MSF10, Jhedup	Circadian behaviour and rythm	(Bloch et al. 2013; Fernandez-Chiappe et al. 2021)
Green (b) and Maroon	anon-WO0118547.80	Melanization-associated	(Bastide et al. 2016)
Green (b) and Maroon	SNX3	Development and morphogenesis	(Zhang et al. 2011)
Green (b) and Maroon	RpS8	Extention of lifespan	(Hoffmann et al. 2013)
Green (b) and Maroon	CG11471	Smell-sensory functions	(Anholt et al. 2001)
Small Brown and Maroon	anon-WO0118547.80	Melanization-associated	(Bastide et al. 2016)

Small Brown and Maroon	Per	Circadian rhythm	(Curtin et al. 1995)
Small Brown and Maroon	LIMK1	Learning and memory formation	(E. A. Nikitina, A. V. Medvedeva, Yu. F. Dolgaya, L. I. Korochkin, G. V. Pavlova & E. V. Savvateeva-Popova 2012)

405

406 The regions with significant genomic divergence yielded some interesting genes (Table
407 1; Supplementary Table 02). Notably, we found genes associated with circadian rhythms in all
408 five comparisons, and genes associated with neuronal functions in four comparisons, and
409 learning and memory formation in three comparisons (Table 1). Interestingly, we found one
410 gene associated with diet (Starch digestion) and another with smell. Two genes were associated
411 with longevity and life-span, and three genes were associated with growth or development
412 (Table 1). Three of the comparisons included melanization-associated genes.

413 Discussion

414 The three main findings of our work are: ***(i)*** The repeated evolution of *Tetragnatha*
415 spiny-leg ecomorphs involves more than a single genomic-basis; ***(ii)*** The genomic-basis of
416 ecomorph differentiation included genes associated with melanization, agreeing with previous
417 ecological and morphological evidence which reported differences in colouration (Gillespie

418 2004; Kennedy et al. 2022); and ***(iii)*** pairwise scans of divergence uncovered evidence for a new
419 axis of differentiation between ecomorphs involving neural and circadian rhythm changes.

420 **Evolutionary history of the *Tetragnatha* spiny-leg clade**

421 Evidence of repeated evolution of ecomorphs comes from the paraphyletic and
422 polyphyletic positioning of ecomorph species in the nuclear whole-genome phylogeny (Figure
423 2), and partitioning of genetic variation in admixture analyses (Figure 3). These analyses show
424 that the spiny-leg radiation can be divided into three large clades. The first clade comprising the
425 lineages in Kaua'i, the oldest island, and including three ecomorphs, namely Green (*T.*
426 *kauaiensis*), Small Brown (*T. mohihi*), and Large Brown (*T. pilosa*). This clade is monophyletic
427 and resolved with high confidence (bootstrap of 100) in the mitochondrial-genome tree (Figure
428 2), corroborating previous results from both nuclear and mitochondrial DNA (Pons and
429 Gillespie 2003; Gillespie 2004). However, the whole-genome data suggests that *T. pilosa* is sister
430 to the remaining radiation, grouping *T. kauaiensis* and *T. mohihi* as its own clade. The branches
431 for *T. kauaiensis*, *T. mohihi* and *T. pilosa* are short, and this could indicate a lower substitution
432 rate, higher missing data, incorrect attachment point of the outgroups, or root misplacement
433 due to artefacts such as low-branch attraction. Lower substitution rate seems the most plausible
434 of these scenarios as missing data can be discarded considering the filtering of the data
435 (Supplementary Table 01). Attachment of outgroups follows the taxonomic knowledge of the
436 group (Kennedy et al. 2022). Root misplacement due to NJ-algorithms, which can be prone to
437 artefacts such as long-branch attraction (Susko et al. 2004), can be indirectly excluded as the
438 UCE-based tree displays a similar topology for these branches and was done using ML. The
439 nuclear-mitochondrial discordance pattern may result from hybridization (Figure 4) and from
440 the fast diversification of the radiation, which can lead to an increase of rates of incomplete
441 lineage sorting (Suh et al. 2015,Cerca et al. 2021b). Evidence for a fast diversification comes
442 from the short branch and the low bootstrap support of the corresponding node (orange circle;
443 Figure 2).

444 The second clade includes the widely distributed Large Brown species *T. quasimodo* and
445 the Small Brown group including *T. obscura*, *T. kukuiki*, *T. kikokiko*, and *T. anuenue*, whose
446 constituent species are present on the islands of Hawai□i, O□ahu, Maui and Moloka□i. The
447 nuclear and the mitochondrial lineages show topological congruence (Figure 2B). The third
448 clade includes a group of Green ecomorph species (*T. tantalus, T. polychromata, T. waikamoi,*
449 and *T. brevignatha*) which are distributed on several islands (Hawai□i, O□ahu, Maui), two
450 separate lineages with Maroon ecomorphs (*T. kamakou* from Moloka□i and Maui; *T. perreirai*
451 from O□ahu), and a Small Brown ecomorph species (*T. restricta*). In this clade, we found
452 evidence for nuclear-mitochondrial disagreements (Figure 2 A-B) and likely hybridization
453 (Figure 4). Most prominently, part of the group comprised by Green ecomorphs, namely *T.*
454 *tantalus* and *T. polychromata*, and the Maroon *T. perreirai*, nests as sister to the second clade in
455 the mitochondrial tree, rendering this clade paraphyletic in the mitochondrial dataset.
456 The Green ecomorph species *Tetragnatha macracantha* (Haleakalā volcano in Maui, and
457 Lana'i) was not included due to the lack of specimens. However, based on previous studies
458 (Gillespie 2004; Cotoras et al. 2018) it clusters with the other Green ecomorph species present
459 in Maui (*T. waikamoi* and the Maui population of *T. brevignatha*). Therefore, the described
460 patterns most likely also include this species. Similarly, *Tetragnatha kukuhaa*, a Small Brown
461 from the Big island is not-included, but it has been previously suggested as a sister to *T. obscura*
462 (Gillespie 2004; Kennedy et al. 2022).
463
464 **Genomic basis of ecomorph evolution**
465 We find evidence that the evolution of ecomorphs has happened repeatedly, in
466 agreement with previous works (Gillespie 2004), and extend these findings by finding evidence
467 that multiple genomic sources underlie repeated phenotypic evolution. Specifically, we find
468 evidence for excess allele sharing, which usually results from hybridization. The strongest signal
469 for hybridization in the dataset, where as much as 10% of the whole-genome variants may be
470 introgressed, occurs from *T. perreirai* to *T. kamakou*, the two species belonging to the Maroon

ecomorph (Figure 4). This evidence is further corroborated by the nuclear-mitochondrial disagreements (Figure 2). Noticeably, *T. perreirai* and *T. kamakou* are not sister species in any of the phylogenetic analysis carried by us (Figure 1; Supplementary Figure 01) and do not currently overlap geographically (*T. perreirai* occurs on the island of O'ahu, *T. kamakou* on Maui and Moloka'i). Several scenarios that could have led to the lack of monophyly of this group in the face of hybridization.

First, introgression may have occurred between *T. perreirai* and an ancestral lineage that was present on Maui or Moloka'i. This introgression event may have carried adaptive alleles associated with the Maroon ecomorph, and opened the Maroon-niche to the admixed lineage, which is now *T. kamakou*. This event of introgression may have been subtle as our exploration of genomic windows for the largest scaffolds (TWISST) and for genomic windows (Fδ ratio) where we found genes associated with melanization (CG8483, anon-WO0118547.80), yielded no evidence for introgression. It is possible that we missed signals of introgression due to the sparsity of low-coverage data along the genome, since missing data may blur genomic patterns and signals (Cerca et al. 2021b). Additionally, we cannot exclude recurrent ancestral hybridization, and this may blury the distinction between hybridization and standing genetic polymorphism (Ferreira et al. 2021). In any case, the admixture analyses suggested no shared ancestry tracks between these three species, even at $K = 15$, and this indicates that signatures of introgression may have been diluted through time.

The second scenario is that the Maroon phenotype evolved first in *T. kamakou*, and was introgressed to O'ahu, leading to the evolution of *T. perreirai*. This alternative scenario implies a back colonization of O'ahu, which is older than Maui Nui. At this stage, we cannot confidently ascertain any of these scenarios, and further data including more genomes, higher coverage, and analyses such as demographic simulations are necessary. We speculate that the combination of ancestral bouts of introgression, fast diversification creating incomplete lineage sorting, changes in population size, population-extinctions as a result of island-cycles, as observed in

497 other adaptive radiations (Meier et al. 2018; De-Kayne et al. 2022), limits our capacity to
498 understand the evolution of this group.

499 We also find evidence of excess allele sharing between members of the Small Brown
500 ecomorph. Namely, there is a signal of hybridization between *T. restricta*, *T. mohihi*, and the
501 clade comprising 4 Small Brown ecomorph species (*T. anuenue*, *T. kukuiki*, *T. obscura*, *T.*
502 *kikokiko*). This signal is particularly clear from the Patterson's D analysis (Supplementary
503 Figure 02), but less clear from the F4 ratio test (Figure 4). This mismatch is likely explained by
504 the different topologies underlying both tests. Two scenarios can explain these results. First,
505 considering that we find evidence for excess lineage sorting between lineages on different
506 islands, it can be speculated that dispersal may have occurred at some time in the past, leading
507 to hybridization. Second, hybridization is not the only cause leading to excess allele sharing and
508 this can confound Patterson's D and F4 -ration analyses. For example, the occurrence of
509 speciation between lineages with different population sizes may cause asymmetries that lead to
510 elevated Patterson's D statistics (smaller populations will have less variants due to the effect of
511 drift). Similarly, if multiple alleles underlie the evolution of an ecomorph, there may be
512 imbalances in allelic variation along the genome, confounding patterns of allele excess. While
513 scenarios of population-size differences and multi-alleles are hard to rule out with low-coverage
514 data, they are unlikely as we also observe mitochondrial-nuclear discordances. Our results
515 contribute to the growing body of work showing that introgression can be a potent force in the
516 passage of adaptive alleles from one lineage to another (Meier et al. 2017; Marques et al. 2019;
517 Sowersby et al. 2021) and can thereby drive repeated phenotypic evolution in the context of an
518 adaptive radiation.

519 Despite the evidence of hybridization in the spiny-leg lineage, hybridization alone is not
520 sufficient to explain the repeated evolution of every ecomorph. Specifically, we do not find
521 evidence for excess allele sharing between the two Green ecomorph clades (*T. kauaiensis* and
522 the clade comprising the lineages *T. brevignatha, T. waikamoi, T. tantalus, T. polychromata*) and
523 a weak signal of hybridization between *T. pilosa* and *T. quasimodo*. The lack of hybridization

within the Green ecomorph is consistent with previous studies, which found no hybridization between Green ecomorph species (Cotoras et al. 2018). The repeated evolution of some ecomorphs may have occurred by either *de novo* mutation or ancestral genetic variation (Barrett and Schluter 2008). Nonetheless, distinguishing between these scenarios benefits from the study of sweeps and coalescence of variants (Barrett and Schluter 2008; Lee and Coop 2017), which would require higher coverage and wider population sampling obtained by us. Despite these limitations, several pieces of evidence may point towards a role of repeated phenotypic evolution of Green and the Large Brown ecomorphs through standing genetic variation. First, the repeated recruitment of variation may be more likely than repeated *de novo* mutations producing the same phenotype (Barrett and Schluter 2008). Second, as discussed above, the phylogenetic reconstruction includes some short branches, which drives higher rates of incomplete lineage sorting, translating into standing genetic variation passing down the lineages. Third, we found 12 genomic regions that were repeatedly significantly-diverged in pairwise F_{ST} comparisons. However, we are careful not to exclude the existence of *de novo* mutation in the radiation and in specific genomic regions, which could be hotspots of mutation with some adaptive value; e.g. (Xie et al. 2019).

Because adaptive introgression seems to play a role in the evolution of some ecomorphs (Small Brown and Maroon), but not in others (Green and Large Brown), this opens the question as to how easy it becomes to re-evolve certain traits without hybridization. In other words, is the transfer of some key genes a strict requirement for the appearance of the Small Brown and Maroon ecomorphs? If that were to be the case, this could explain why the Maroon ecomorph is entirely absent from Lana'i and the Big Island (Gillespie 2004).

Ecological and genomic drivers of ecomorph evolution

Spiny-leg *Tetragnatha* spiders are largely confined to mid-elevation wet and mesic forests on Hawaiian volcanoes (1,200-1,800 meters) and diversification has occurred largely within this environment (Hiller et al. 2019). This suggests that, in addition to the physical barrier between islands imposed by the ocean, the lowland area may act as a strong isolating

551 barrier, as has been shown for many taxa in more stable environments (Janzen 1967). The
552 spiders' forest habitats have mosaic distributions, and it is likely that the separation between
553 them has triggered a dynamic interplay between natural selection in response to micro-habitat
554 availability and allopatric divergence (Vandergast et al. 2004; Roderick et al. 2012; Cotoras et al.
555 2018). In particular, ecomorph divergence is likely due to allopatric establishment on different
556 islands and volcanoes, followed by secondary contact, competition between ecologically similar
557 species and hence the accumulation of divergence (Schluter 2000; Cotoras et al. 2018).
558 Dispersal and secondary contact of diverged populations may have led to a macroevolutive
559 ecological character displacement and the evolution of particular ecomorphologies. This
560 scenario is consistent with the evidence for hybridization at various points of the radiation,
561 which suggests that dispersal may have occurred multiple times across the phylogeny, leading
562 to the introgression of variants.

563 A major goal of adaptive radiation research is to disentangle the ecological drivers of
564 species formation (speciation) and adaptation to the environment (local adaptation). Previous
565 research has suggested that ecomorph-colouration has been associated with selective pressure
566 from predators (Gillespie 2004). In the current study, F_{ST} comparisons uncovered melanization
567 genes in regions of genomic divergence, which agree with the natural history observations of
568 the group and the colour-characterization of the ecomorphs. Interestingly, we also find evidence
569 for genes associated with circadian rhythms, neuronal and synaptic activity genes, life span,
570 learning and memory formation, which can be seen as an unexplored axis of physiological and
571 ecological differentiation. Specifically, these genes may indicate that ecomorph-evolution may
572 involve more phenotypic changes than shifts in coloration and micro-habitat use. For example,
573 circadian rhythm genes are found across the tree of life and are important for a wide array of
574 functions, from allowing organisms to synchronise with their immediate environment to
575 regulating reproductive activity, and it has been suggested that they play an important role in
576 environmental adaptation (Yerushalmi and Green 2009). Finally, the evidence for genomic
577 differentiation in developmental genes may suggest that shifts in developmental stages may

have an important function in the *Tetragnatha* spiny-leg adaptive radiation. This is consistent with previous work which shows that the initial appearance of the Maroon ecomorph is associated with developmental shifts in coloration on the oldest island of Kauai (Brewer et al. 2014), by identifying several genes under selection likely responsible for changes in coloration and developmental processes – reticulon nogo and apolipoprotein d.

Conclusion

The whole-genome sequencing of *Tetragnatha* spiny-leg ecomorphs showed that the genomic basis of repeated ecomorph evolution is multifarious even in closely related species, as some ecomorphs likely arose through hybridization (Small Brown, Maroon), while others likely arose by shared standing genetic variation or *de novo* mutation (Green, large Brown). We also found that ecomorph evolution in the spiny-legs may go beyond their colouration, as regions with high genomic divergence consistently pointed to genes associated with other potential ecological axes of differentiation, such as learning and memory formation, circadian rhythms, and developmental shifts. However, it is likely that a complex evolutionary history involving population extinctions, population structuring and ghost-lineages blurry the reconstruction and interpretation of evolutionary patterns.

Author Contributions

JC, THS, RGG obtained funding. JC and RGG designed the study. RGG, DDC, SK, HK, AJW provided samples. JC, LH generated the data. JC analysed the data with contributions on scripting and interpreting the data from CGS, VCB, JM, DDC, JML, CFP and DD. JC drafted a first manuscript, and all the authors contributed to the writing and clarity of the manuscript.

Data Accessibility

Data is being made available through ENA XXX. Code is at github José.

Acknowledgements

The authors would like to acknowledge a large number of people and institutions that collaborated at different stages of this research. The fieldwork in Maui Nui was supported by Timothy Bailey and William Roderick. JC is grateful to Mike Martin for access to a super computer cluster, Mark Ravinet for his constant mentorship and LD scripts, and Michael Matschiner for comments on the manuscript. We are grateful to Jun Ying Lim for providing samples.

The permit processing and access to different reserves and private land was possible thanks to Pat Bily (TNC Maui), Lance DaSilva (DOFAW Maui), Danae Dean (Kahoma Ranch), Charmian Dang (NAR), the late Betsy Gagne (NAR), Elizabeth Gordon (HALE), Paula Hartzell (Lana□i Resorts, LLC), Pomaika□i Kaniaupio-Crozier (Maui Land and Pineapple), Cynthia King (DLNR), Peter Landon (NAR Maui), Russell Kallstrom and Ed Misaki (TNC Moloka□i) and Joe Ward (Maui Land and Pineapple).

JC, RG, THS were supported by a Peder Sather grant, DDC was supported by a Fulbright/CONICYT doctoral fellowship, Integrative Biology department and the Graduate Division of UC Berkeley, the Margaret C. Walker fund (Essig Museum of Entomology) and a Humboldt postdoctoral fellowship. Fieldwork was funded by NSF grants DEB 1241253 and DEB 1927510 to RG.

References

Andrews, S. 2017. FastQC: a quality control tool for high throughput sequence data. 2010.

Anholt, R. R., J. J. Fanara, G. M. Fedorowicz, I. Ganguly, N. H. Kulkarni, T. F. Mackay, and S. M. Rollmann. 2001. Functional genomics of odor-guided behavior in Drosophila melanogaster. Chem. Senses 26:215–221.

626 Barrett, R. D. H., and D. Schluter. 2008. Adaptation from standing genetic variation. Trends Ecol. Evol.
627 23:38–44.
628 Bastide, H., J. D. Lange, J. B. Lack, A. Yassin, and J. E. Pool. 2016. A Variable Genetic Architecture of
629 Melanic Evolution in Drosophila melanogaster. Genetics 204:1307–1319.
630 Bloch, G., E. Hazan, and A. Rafaeli. 2013. Circadian rhythms and endocrine functions in adult insects.
631 J. Insect Physiol. 59:56–69.
632 Bolger, A. M., M. Lohse, and B. Usadel. 2014. Trimmomatic: a flexible trimmer for Illumina sequence
633 data. Bioinformatics 30:2114–2120.
634 Bradley, S., S. Narayanan, and M. Rosbash. 2012. NAT1/DAP5/p97 and atypical translational control
635 in the Drosophila Circadian Oscillator. Genetics 192:943–957.
636 Brewer, M. S., D. D. Cotoras, P. J. P. Croucher, and R. G. Gillespie. 2014. New sequencing technologies,
637 the development of genomics tools, and their applications in evolutionary arachnology.
638 Arachnol. Mitt. 42:1–15. American Arachnological Society.
639 Cerca, J. 2022. A simple conceptual framework and nomenclature for studying repeated, parallel and
640 convergent evolution. EcoEvoRxiv.
641 Cerca, J., E. E. Armstrong, J. Vizueta, R. Fernández, D. Dimitrov, B. Petersen, S. Prost, J. Rozas, D.
642 Petrov, and R. G. Gillespie. 2021a. The Tetragnatha kauaiensis Genome Sheds Light on the
643 Origins of Genomic Novelty in Spiders. Genome Biol. Evol. 13.
644 Cerca, J., A. G. Rivera-Colón, M. S. Ferreira, M. Ravinet, M. D. Nowak, J. M. Catchen, and T. H. Struck.
645 2021b. Incomplete lineage sorting and ancient admixture, and speciation without morphological
646 change in ghost-worm cryptic species. PeerJ 9:e10896.
647 Choi, J. Y., X. Dai, O. Alam, J. Z. Peng, P. Rughani, S. Hickey, E. Harrington, S. Juul, J. F. Ayroles, M. D.
648 Purugganan, and E. A. Stacy. 2021. Ancestral polymorphisms shape the adaptive radiation of
649 Metrosideros across the Hawaiian Islands. Proc. Natl. Acad. Sci. U. S. A. 118.
650 Cotoras, D. D., K. Bi, M. S. Brewer, D. R. Lindberg, S. Prost, and R. G. Gillespie. 2018. Co-occurrence of
651 ecologically similar species of Hawaiian spiders reveals critical early phase of adaptive
652 radiation. BMC Evol. Biol. 18:100.

653 Curtin, K. D., Z. J. Huang, and M. Rosbash. 1995. Temporally regulated nuclear entry of the Drosophila
654 period protein contributes to the circadian clock. Neuron 14:365–372.
655 Danecek, P., J. K. Bonfield, J. Liddle, J. Marshall, V. Ohan, M. O. Pollard, A. Whitwham, T. Keane, S. A.
656 McCarthy, R. M. Davies, and H. Li. 2021. Twelve years of SAMtools and BCFtools. Gigascience 10.
657 De-Kayne, R., O. M. Selz, D. A. Marques, D. Frei, O. Seehausen, and P. G. D. Feulner. 2022. Genomic
658 architecture of adaptive radiation and hybridization in Alpine whitefish. Nat. Commun. 13:4479.
659 Dierckxsens, N., P. Mardulyn, and G. Smits. 2017. NOVOPlasty: de novo assembly of organelle
660 genomes from whole genome data. Nucleic Acids Res. 45:e18.
661 E. A. Nikitina, A. V. Medvedeva, Yu. F. Dolgaya, L. I. Korochkin, G. V. Pavlova & E. V. Savvateeva-
662 Popova. 2012. Involvement of GDNF and LIMK1 and heat shock proteins in drosophila learning
663 and memory formation. Journal of Evolutionary Biochemistry and Physiology volume, doi:
664 10.1134/S0022093012050076.
665 Emms, D. M., and S. Kelly. 2015. OrthoFinder: solving fundamental biases in whole genome
666 comparisons dramatically improves orthogroup inference accuracy. Genome Biol. 16:157.
667 Evanno, G., S. Regnaut, and J. Goudet. 2005. Detecting the number of clusters of individuals using the
668 software STRUCTURE: a simulation study. Mol. Ecol. 14:2611–2620.
669 Faircloth, B. C. 2016. PHYLUCE is a software package for the analysis of conserved genomic loci.
670 Bioinformatics 32:786–788.
671 Fernandez-Chiappe, F., L. Frenkel, C. C. Colque, A. Ricciuti, B. Hahm, K. Cerredo, N. I. Muraro, and M. F.
672 Ceriani. 2021. High-Frequency Neuronal Bursting is Essential for Circadian and Sleep Behaviors
673 in Drosophila. J. Neurosci. 41:689–710.
674 Ferreira, M. S., M. R. Jones, C. M. Callahan, L. Farelo, Z. Tolesa, F. Suchentrunk, P. Boursot, L. S. Mills, P.
675 C. Alves, J. M. Good, and J. Melo-Ferreira. 2021. The Legacy of Recurrent Introgression during the
676 Radiation of Hares. Syst. Biol. 70:593–607.
677 Garcia-Erill, G., M. M. Kjaer, A. Albrechtsen, H. R. Siegismund, and R. Heller. 2021. Vicariance followed
678 by secondary gene flow in a young gazelle species complex. Mol. Ecol. 30:528–544.

679 Ghosh, A. 2013. Timing, growth and homeostasis: An anthology of three novel players in Drosophila
680 melanogaster. search.proquest.com.
681 Gillespie, R. 2004. Community assembly through adaptive radiation in Hawaiian spiders. Science
682 303:356–359.
683 Gillespie, R. G. 2016. Island time and the interplay between ecology and evolution in species
684 diversification. Evol. Appl. 9:53–73.
685 Gillespie, R. G., S. P. Benjamin, M. S. Brewer, M. A. J. Rivera, and G. K. Roderick. 2018. Repeated
686 Diversification of Ecomorphs in Hawaiian Stick Spiders. Curr. Biol. 28:941–947.e3.
687 Gillespie, R. G., G. M. Bennett, L. De Meester, J. L. Feder, R. C. Fleischer, L. J. Harmon, A. P. Hendry, M. L.
688 Knope, J. Mallet, C. Martin, C. E. Parent, A. H. Patton, K. S. Pfennig, D. Rubinoff, D. Schluter, O.
689 Seehausen, K. L. Shaw, E. Stacy, M. Stervander, J. T. Stroud, C. Wagner, and G. O. U. Wogan. 2020.
690 Comparing Adaptive Radiations Across Space, Time, and Taxa. J. Hered. 111:1–20.
691 Guan, Z., S. Saraswati, B. Adolfsen, and J. T. Littleton. 2005. Genome-wide transcriptional changes
692 associated with enhanced activity in the Drosophila nervous system. Neuron 48:91–107.
693 Hevia, C. F., A. López-Varea, N. Esteban, and J. F. de Celis. 2017. A Search for Genes Mediating the
694 Growth-Promoting Function of TGFβ in the Drosophila melanogaster Wing Disc. Genetics
695 206:231–249.
696 Hiller, A. E., M. S. Koo, and K. R. Goodman. 2019. Niche conservatism predominates in adaptive
697 radiation: comparing the diversification of Hawaiian arthropods using ecological niche
698 modelling. Biol. J. Linn. Soc. Lond. academic.oup.com.
699 Hoffmann, J., R. Romey, C. Fink, L. Yong, and T. Roeder. 2013. Overexpression of Sir2 in the adult fat
700 body is sufficient to extend lifespan of male and female Drosophila. Aging 5:315–327.
701 Ibrahim, D. M., B. Biehs, T. B. Kornberg, and A. Klebes. 2013. Microarray comparison of anterior and
702 posterior Drosophila wing imaginal disc cells identifies novel wing genes. G3 3:1353–1362.
703 Janzen, D. H. 1967. Why Mountain Passes are Higher in the Tropics. Am. Nat. 101:233–249. The
704 University of Chicago Press.

705 Katoh, K., and D. M. Standley. 2013. MAFFT multiple sequence alignment software version 7:
706 improvements in performance and usability. Mol. Biol. Evol. 30:772–780.
707 Kennedy, S. R., J. Y. Lim, S. A. Adams, H. Krehenwinkel, and R. G. Gillespie. 2022. What is adaptive
708 radiation? Many manifestations of the phenomenon in an iconic lineage of Hawaiian spiders.
709 Mol. Phylogenet. Evol. 175:107564.
710 Koch, I., H. Schwarz, D. Beuchle, B. Goellner, M. Langegger, and H. Aberle. 2008. Drosophila ankyrin 2
711 is required for synaptic stability. Neuron 58:210–222.
712 Kopelman, N. M., J. Mayzel, M. Jakobsson, N. A. Rosenberg, and I. Mayrose. 2015. Clumpak: a program
713 for identifying clustering modes and packaging population structure inferences across K. Mol.
714 Ecol. Resour. 15:1179–1191.
715 Kousathanas, A., C. Leuenberger, V. Link, C. Sell, J. Burger, and D. Wegmann. 2017. Inferring
716 Heterozygosity from Ancient and Low Coverage Genomes. Genetics 205:317–332.
717 Lee, K. M., and G. Coop. 2017. Distinguishing Among Modes of Convergent Adaptation Using
718 Population Genomic Data. Genetics 207:1591–1619.
719 Lee, K. M., and G. Coop. 2019. Population genomics perspectives on convergent adaptation. Philos.
720 Trans. R. Soc. Lond. B Biol. Sci. 374:20180236.
721 Lefort, V., R. Desper, and O. Gascuel. 2015. FastME 2.0: A Comprehensive, Accurate, and Fast
722 Distance-Based Phylogeny Inference Program. Mol. Biol. Evol. 32:2798–2800.
723 Liebl, F. L. W., K. M. Werner, Q. Sheng, J. E. Karr, B. D. McCabe, and D. E. Featherstone. 2006. Genome-
724 wide P-element screen for Drosophila synaptogenesis mutants. J. Neurobiol. 66:332–347.
725 Li, H., and R. Durbin. 2009. Fast and accurate short read alignment with Burrows–Wheeler
726 transform. Bioinformatics 25:1754–1760. Oxford Academic.
727 Li, H., B. Handsaker, A. Wysoker, T. Fennell, J. Ruan, N. Homer, G. Marth, G. Abecasis, R. Durbin, and
728 1000 Genome Project Data Processing Subgroup. 2009. The Sequence Alignment/Map format
729 and SAMtools. Bioinformatics 25:2078–2079.
730 Losos, J. B. 2010. Adaptive radiation, ecological opportunity, and evolutionary determinism.
731 American Society of Naturalists E. O. Wilson award address. Am. Nat. 175:623–639.

732 Losos, J. B. 2011. Convergence, adaptation, and constraint. Evolution 65:1827–1840.

733 Losos, J. B., and R. E. Ricklefs. 2009. Adaptation and diversification on islands. Nature 457:830–836.

734 Malinsky, M., M. Matschiner, and H. Svardal. 2021. Dsuite - Fast D-statistics and related admixture
735 evidence from VCF files. Mol. Ecol. Resour. 21:584–595. Wiley.

736 Malinsky, M., H. Svardal, A. M. Tyers, E. A. Miska, M. J. Genner, G. F. Turner, and R. Durbin. 2018.
737 Whole-genome sequences of Malawi cichlids reveal multiple radiations interconnected by gene
738 flow. Nat Ecol Evol 2:1940–1955.

739 Marques, D. A., K. Lucek, V. C. Sousa, L. Excoffier, and O. Seehausen. 2019. Admixture between old
740 lineages facilitated contemporary ecological speciation in Lake Constance stickleback. Nat.
741 Commun. 10:4240.

742 Masonick, P., A. Meyer, and C. D. Hulsey. 2022. Phylogenomic Analyses Show Repeated Evolution of
743 Hypertrophied Lips Among Lake Malawi Cichlid Fishes. Genome Biol. Evol. 14.

744 Mattila, J., and V. Hietakangas. 2017. Regulation of Carbohydrate Energy Metabolism in Drosophila
745 melanogaster. Genetics 207:1231–1253.

746 McKenna, A., M. Hanna, E. Banks, A. Sivachenko, K. Cibulskis, A. Kernytsky, K. Garimella, D. Altshuler,
747 S. Gabriel, M. Daly, and M. A. DePristo. 2010. The Genome Analysis Toolkit: a MapReduce
748 framework for analyzing next-generation DNA sequencing data. Genome Res. 20:1297–1303.

749 Meier, J. I., D. A. Marques, S. Mwaiko, C. E. Wagner, L. Excoffier, and O. Seehausen. 2017. Ancient
750 hybridization fuels rapid cichlid fish adaptive radiations. Nat. Commun. 8:14363.

751 Meier, J. I., D. A. Marques, C. E. Wagner, L. Excoffier, and O. Seehausen. 2018. Genomics of Parallel
752 Ecological Speciation in Lake Victoria Cichlids.

753 Meirmans, P. G. 2015. Seven common mistakes in population genetics and how to avoid them. Mol.
754 Ecol. 24:3223–3231.

755 Nazario-Toole, A. E., J. Robalino, K. Okrah, H. Corrada-Bravo, S. M. Mount, and L. P. Wu. 2018. The
756 Splicing Factor RNA-Binding Fox Protein 1 Mediates the Cellular Immune Response in
757 Drosophila melanogaster. J. Immunol. 201:1154–1164.

758 Paaby, A. B., and P. S. Schmidt. 2009. Dissecting the genetics of longevity in Drosophila melanogaster.
759 Fly 3:29–38.
760 Paradis, E., K. Strimmer, J. Claude, G. Jobb, R. Opgen-Rhein, J. Dutheil, Y. Noel, B. Bolker, and J. Lemon.
761 2008. The ape package. Analyses of phylogenetics and evolution.
762 Patterson, N., P. Moorjani, Y. Luo, S. Mallick, N. Rohland, Y. Zhan, T. Genschoreck, T. Webster, and D.
763 Reich. 2012. Ancient admixture in human history. Genetics 192:1065–1093.
764 Pease, J. B., D. C. Haak, M. W. Hahn, and L. C. Moyle. 2016. Phylogenomics Reveals Three Sources of
765 Adaptive Variation during a Rapid Radiation. PLoS Biol. 14:e1002379.
766 Pons, J., and R. G. Gillespie. 2003. Common origin of the satellite DNAs of the Hawaiian spiders of the
767 genus Tetragnatha: evolutionary constraints on the length and nucleotide composition of the
768 repeats. Gene 313:169–177.
769 Proshkina, E. N., M. V. Shaposhnikov, A. F. Sadritdinova, A. V. Kudryavtseva, and A. A. Moskalev. 2015.
770 Basic mechanisms of longevity: A case study of Drosophila pro-longevity genes. Ageing Res. Rev.
771 24:218–231.
772 Purcell, S., B. Neale, K. Todd-Brown, L. Thomas, M. A. R. Ferreira, D. Bender, J. Maller, P. Sklar, P. I. W.
773 de Bakker, M. J. Daly, and P. C. Sham. 2007. PLINK: a tool set for whole-genome association and
774 population-based linkage analyses. Am. J. Hum. Genet. 81:559–575.
775 Quinlan, A. R., and I. M. Hall. 2010. BEDTools: a flexible suite of utilities for comparing genomic
776 features. Bioinformatics 26:841–842.
777 Ravinet, M., R. Faria, R. K. Butlin, J. Galindo, N. Bierne, M. Rafajlović, M. A. F. Noor, B. Mehlig, and A. M.
778 Westram. 2017. Interpreting the genomic landscape of speciation: a road map for finding
779 barriers to gene flow. J. Evol. Biol. 30:1450–1477.
780 Roderick, G. K., P. J. P. Croucher, A. G. Vandergast, and R. G. Gillespie. 2012. Species Differentiation on
781 a Dynamic Landscape: Shifts in Metapopulation Genetic Structure Using the Chronology of the
782 Hawaiian Archipelago. Evol. Biol. 39:192–206.
783 Salzburger, W. 2018. Understanding explosive diversification through cichlid fish genomics. Nat. Rev.
784 Genet. 19:705–717.

785 Schluter, D. 2000. The Ecology of Adaptive Radiation. OUP Oxford.

786 Schubert, M., S. Lindgreen, and L. Orlando. 2016. AdapterRemoval v2: rapid adapter trimming,
787 identification, and read merging. BMC Res. Notes 9:88.

788 Skotte, L., T. S. Korneliussen, and A. Albrechtsen. 2013. Estimating individual admixture proportions
789 from next generation sequencing data. Genetics 195:693–702.

790 Sowersby, W., J. Cerca, B. B. M. Wong, T. K. Lehtonen, D. G. Chapple, M. Leal-Cardín, M. Barluenga, and
791 M. Ravinet. 2021. Pervasive admixture and the spread of a large-lipped form in a cichlid fish
792 radiation. Mol. Ecol. 30:5551–5571.

793 Stern, D. L. 2013. The genetic causes of convergent evolution. Nat. Rev. Genet. 14:751–764.

794 Suh, A., L. Smeds, and H. Ellegren. 2015. The Dynamics of Incomplete Lineage Sorting across the
795 Ancient Adaptive Radiation of Neoavian Birds. PLoS Biol. 13:e1002224.

796 Susko, E., Y. Inagaki, and A. J. Roger. 2004. On inconsistency of the neighbor-joining, least squares,
797 and minimum evolution estimation when substitution processes are incorrectly modeled. Mol.
798 Biol. Evol. 21:1629–1642.

799 Urban, S., J. Gerwin, C. D. Hulsey, A. Meyer, and C. F. Kratochwil. 2022. The repeated evolution of
800 stripe patterns is correlated with body morphology in the adaptive radiations of East African
801 cichlid fishes. Ecol. Evol. 12:e8568.

802 Vandergast, A. G., R. G. Gillespie, and G. K. Roderick. 2004. Influence of volcanic activity on the
803 population genetic structure of Hawaiian Tetragnatha spiders: fragmentation, rapid population
804 growth and the potential for accelerated evolution. Mol. Ecol. 13:1729–1743.

805 Vieira, F. G., F. Lassalle, T. S. Korneliussen, and M. Fumagalli. 2015. Improving the estimation of
806 genetic distances from Next-Generation Sequencing data. Biol. J. Linn. Soc. Lond. 117:139–149.
807 Oxford Academic.

808 Volkenhoff, A., A. Weiler, M. Letzel, M. Stehling, C. Klämbt, and S. Schirmeier. 2015. Glial Glycolysis Is
809 Essential for Neuronal Survival in Drosophila. Cell Metab. 22:437–447.

Wu, X., R. Li, Q. Li, H. Bao, and C. Wu. 2016. Comparative transcriptome analysis among parental inbred and crosses reveals the role of dominance gene expression in heterosis in Drosophila melanogaster. Sci. Rep. 6:21124.

Xie, K. T., G. Wang, A. C. Thompson, J. I. Wucherpfennig, T. E. Reimchen, A. D. C. MacColl, D. Schluter, M. A. Bell, K. M. Vasquez, and D. M. Kingsley. 2019. DNA fragility in the parallel evolution of pelvic reduction in stickleback fish. Science 363:81–84.

Yang, C.-P., T. J. Samuels, Y. Huang, L. Yang, D. Ish-Horowicz, I. Davis, and T. Lee. 2017. Imp and Syp RNA-binding proteins govern decommissioning of Drosophila neural stem cells. Development 144:3454–3464.

Yerushalmi, S., and R. M. Green. 2009. Evidence for the adaptive significance of circadian rhythms. Ecol. Lett. 12:970–981.

Zhang, P., Y. Wu, T. Y. Belenkaya, and X. Lin. 2011. SNX3 controls Wingless/Wnt secretion through regulating retromer-dependent recycling of Wntless. Cell Res. 21:1677–1690.